Michigan State University

National Superconducting Cyclotron Laboratory

SINGLE-PARTICLE BEAM DYNAMICS STUDIES FOR THE UNIVERSITY OF MARYLAND ELECTRON RING

L.G. VOROBIEV, X. WU and R.C. YORK

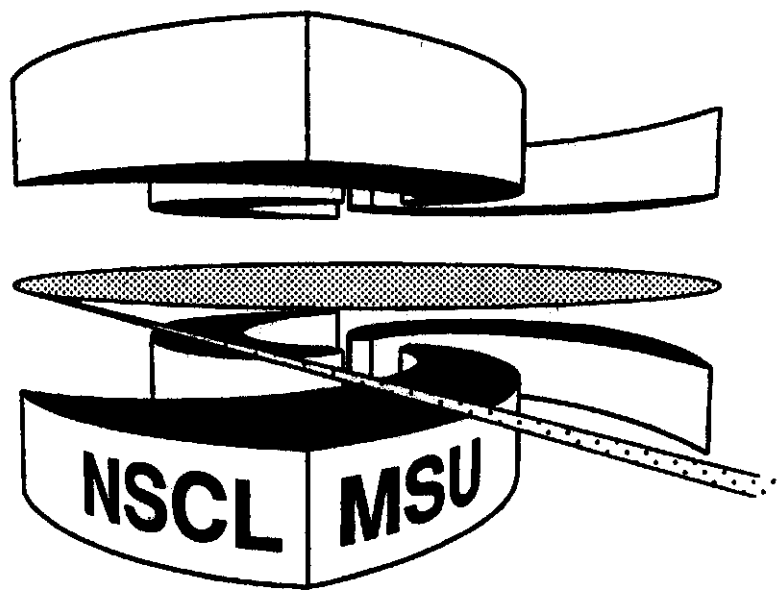

MSUCL-1114 SEPTEMBER 1998

Single-Particle Beam Dynamics Studies for the University of Maryland Electron Ring

L.G. Vorobiev, X. Wu and R.C. York

NSCL, Michigan State University, East Lansing, MI 48824

Abstract

A detailed single particle analysis of the University of Maryland Electron Ring project was performed. For this analysis a lattice working point of ν_x=7.78, ν_y =7.70 was chosen to avoid all resonances up to the 4' order. Higher order multipole terms of the dipole magnets and quadrupole lenses were included in the analysis. The influence of the Earth's magnetic field was balanced by Helmholtz-like wires and the effects of mechanical misalignments were corrected by short dipoles (correctors) together with adjustment of the lattice dipoles. The number of beam positions monitors (BPMs) used in the orbit correction simulations was minimized to 15. Magnet mispowering studies showed that the closed orbit distortions (dipole effect) are within acceptable limits. Changes to the tune shift and lattice functions due to mispowering (quadrupole effect) were acceptable as well. The studies show that the chosen lattice is adequate for the ring operation.

1. INTRODUCTION

The goal of the Electron-Ring project is the construction of a compact, low-energy electron ring operating with very high current electron beams. [1] Experiments with this facility should help improve our understanding of space charge dominated beam phenomena, and thus, support practical designs for projects such as Heavy Ion Driven Inertial Fusion (HIDIF) and other advanced accelerator applications.

A necessary (but by no means sufficient) condition for the E-Ring is reliable operation at zero current. Thus, our present work is concentrated on single particle analysis. We evaluated the lattice working point, the influence of magnet multipoles on beam dynamics, compensation of the Earth's magnetic field, as well as correction of effects due to mechanical misalignment. We also considered the effects of magnet mispowering and an alternate lattice-operating mode, which may facilitate the orbit correction scheme. The computational tool we have used is the DIMAD code.. [2]

Ring Layout. The Electron Ring has a circumference of 11.52 m and an injected beam rigidity of 3.389 gauss·m. There are 36 dipole magnets (each bending 10°) and 72 quadrupole lenses. The one cell structure is FODO with the E-Ring consisting of 36 cells. A general layout of the E-Ring is shown in Figure 1.

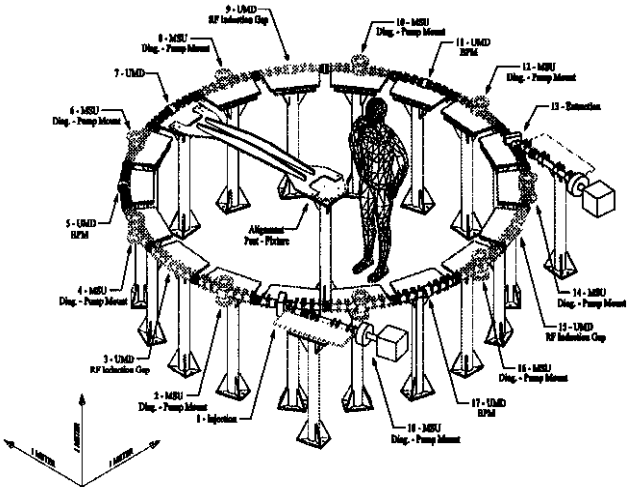

Figure 1. E-Ring layout.

2. LATTICE WORKING POINT

Tune Diagram. According to preliminary estimates of the E-Ring design parameters, the focusing structure should have a phase advance of about 76" per cell for a zero current beam. Plotted in Figure 2 is the working point (ν_x= 7.78 and ν_y= 7.70) chosen to avoid all resonances up to 4^{th} order in the vicinity of $\nu_{x,\,y}$. The space charge tune shift estimated for full current will be about $\Delta\nu \approx 6.0$, (see ref. [1]) and the working point will drift through many resonances. However, this issue is not included in the present analysis, but rather will be a topic of further detailed studies.

Machine functions for a cell. Given the chosen $\nu_{x,y}$, machine functions of the E-Ring from DIMAD are shown in Figure 3 where the Twiss functions and dispersion are plotted for one segment (= two cells). The matched machine functions are: β_x =0.261 m, α_x z-1.31, β_y=0.264

m, α_y= +1.32, η_x = 0.0358 m, η'_x = 0.1447. Figure 4 illustrates the phase advance functions for one segment where ν_x=0.4322, ν_y=0.4278 (Correspondingly ν_x=0.2161 and ν_y=0.2139 for one cell).

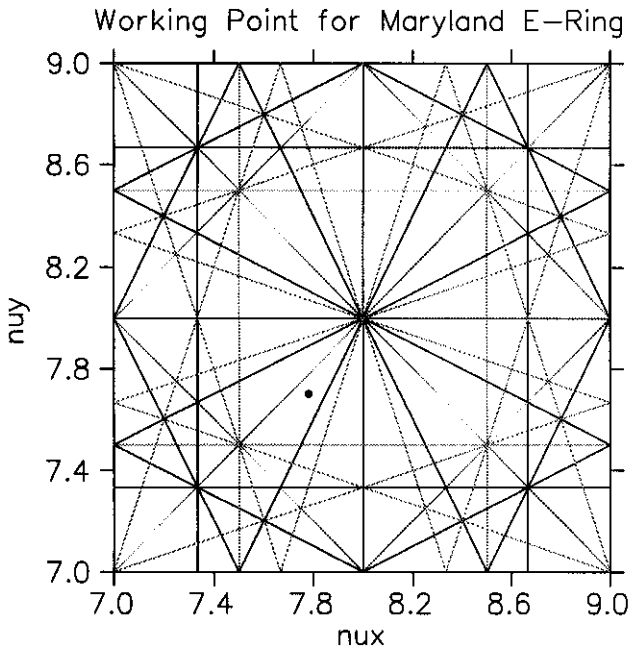

Figure 2. The working point in the resonance plane.

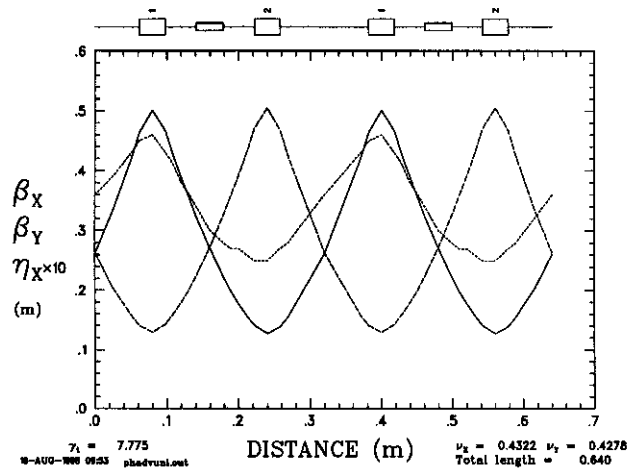

Figure 3. Machine functions (βx – solid, βy - dashed, ηx - dots) for one segment (2 cells).

Smear. To check the choice of the working point, a quantitative criterion - "the smear factor" - was used to estimate the effective phase volume dilution after multi-turn tracking.

Single particle tracking (typically 1000 turns) with DIMAD produced a data array of phase coordinates (x, x', y, y') after every turn. The Courant-Snyder invariants for each turn was then calculated from the machine functions and the phase coordinates at that point. The array of these invariants was then processed [3] and the maximum ($A^{max}_{x,y}$), minimum ($A^{min}_{x,y}$), and mean ($A^{mean}_{x,y}$) invariant values were found. The smear factors for the horizontal and vertical planes were calculated from:

$$S_{x,y} = \frac{A^{max}_{x,y} - A^{min}_{x,y}}{A^{mean}_{x,y}}$$

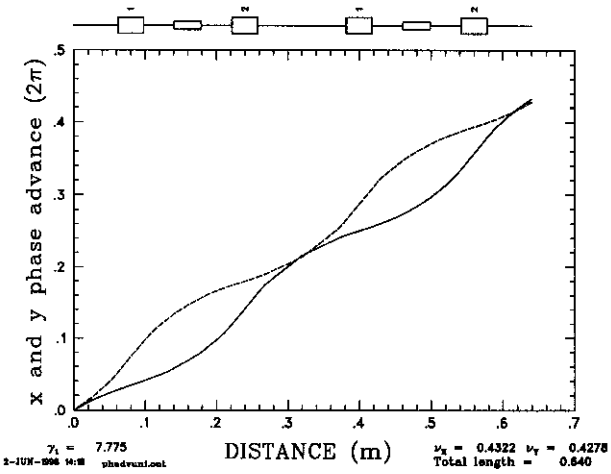

Figure 4. Phase advances (ϕx – solid, ϕy – dashed) within one segment (2 cells).

For purely linear motion, the smear value is equal zero. In the presence of non-linear terms and/or mechanical misalignments, mispowering etc. the smear increases. For DIMAD tracking to 2nd order, the total smear increase in both planes for the unperturbed lattice was below 1.5% for an emittance of 10 π mm-mrad.

3. MAGNET MULTIPOLES

All the ring magnetic elements will be fabricated using "printed-circuit" technology. [1] Magnetic measurement data for the dipoles and quadrupoles were obtained from the University of Maryland and included in the optics analysis. The magnetic measurements were performed for R=15/16 inch = 2.381 cm.

In the tracking, we assumed that all allowed multipoles were systematic (errors due to elements fabrication), whereas all errors corresponding to non-allowed multipoles (errors due to focusing structure assembling) were random.

Dipole multipole analysis. The magnetic field in the bending magnet may be represented by the power expansion:

$$B^D = B\rho \sum_{n=0}^{n=4} K_n^D x^n$$

Where Bρ (3.389 gauss·m) is the beam magnetic rigidity and K_n^D are the expansion coefficients. The value

$K_0^D = B_0^D / B\rho = 4.64$ [1/m] (with $B_0^D = 15.728$ gauss and an effective length of 37.6 mm providing a 10° bend).

All other coefficients for n>1 are given by:

$$K_n^D = K_0^D B_n^D / (B_0^D R).$$

The ratios B_n^D / B_0^D are listed in Table 1.

N	Amplitude B_n^D / B_θ^D	K_n^D	Type
1	0.076%	1.481e+00	Random
2	2.00%	1.637e+02	Systematic
3	0.00%	0	Random
4	0.49%	7.074e+04	Systematic

Table 1. Dipole multipole measurements.

Quadrupole multipole analysis. For the magnetic field of a quadrupole, we use a similar representation:

$$B^Q = B\rho \sum_{n=1}^{n=5} K_n^Q x^n$$

The value $K_1^Q = 227$ [1/m^2] was found from lattice fitting, and since $B_1^Q = B\rho K_1^Q R$ and $B_n^Q = B\rho K_n^Q R^n$, all coefficients for n > 1 are given by:

$$K_n = K_1^Q B_n^Q / (R^{n-1} B_1)$$

The quadrupole multipole values are listed in Table 2.

N	Amplitude B_n^Q / B_1^Q	K_n^Q	Type
2	1.00%	1.737e+00	Random
3	0.30%	2.188e+02	Random
4	0.56%	1.715e+00	Random
5	0.112%	7.940e+05	Systematic

Table 2. Quadrupole multipole analysis.

Smear from Magnet Multipoles. The smear factor was used to estimate the influence of the higher-order multipoles on the beam dynamics of the E-Ring. All random errors were assumed to have a Gaussian distribution with 1σ corresponding to the value of the coefficients K_n^Q for the random terms. The values for the systematic terms were fixed at the values given since their contribution to smear was found negligible even for several times the measured values. (See Tables 1 and 2).

The smear ($S_{x,y}$) was evaluated as a function of the multipole strength by taking the σ value for the Gaussian distribution to be 1, 2, 3, or 4 times the values given in Table 1 and Table 2. Shown in Figure 5 is the smear versus the scaled sigma values. Even for random errors three times that measured, the smear is still below 5% after 1000-turn tracking for a beam of emittance 10 π mm-mrad. Hence, the measured dipole and quadrupole multipoles are adequate for the ring operation.

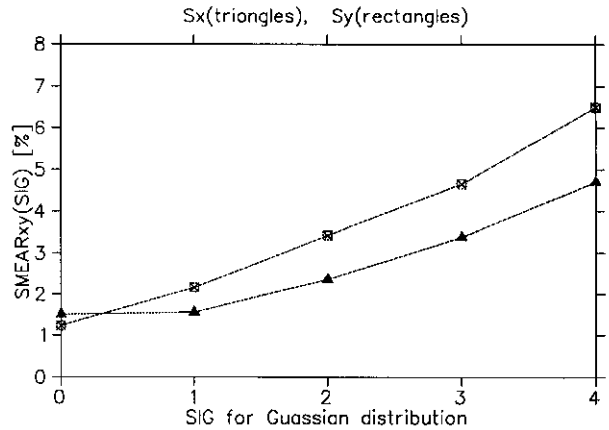

Figure 5. Smear factor after 1000 turns as a function of the amplitude of the random errors.

We found that random errors (non-allowed poles) are the major contributors to smear growth with the systematic errors providing minor contributions to the smear. The largest contributions were due to K_1^B (the quadrupole component in the dipoles) and to K_1^Q (the sextupole component in the quadrupoles).

4. EARTH'S MAGNETIC FIELD AND CORRECTIONS

The Earth's magnetic field in the vicinity of the ring was measured by the University of Maryland group. For the tracking analysis, we have used for the Earth's magnetic field the following analytical representation (See. **Fig. 6**):

$B_r = 0.225 \sin\theta$ [gauss] (for the radial field)
$B_z = -0.55 \equiv$ const [gauss] (for the vertical field)

The effect of this magnetic field was represented by 13 kicks per segment or 234 kicks around the ring. The Earth's vertical field was compensated by adjustment of the 36 ring dipole magnets. The Earth's radial field was compensated by 18 segments of Helmholtz-like conductors with maximum current required for these conductors about of 4.6 A. Under these conditions (the multipole values of Table 1 and Table 2 are included), the analysis of the closed orbit distortion after compensation resulted in:

$$\mathbf{x_{rms} = 0.508\ mm,\ y_{rms} = 0.167\ mm}$$
$$\mathbf{x_{max} = 0.868\ mm,\ y_{max} = 0.453\ mm}$$

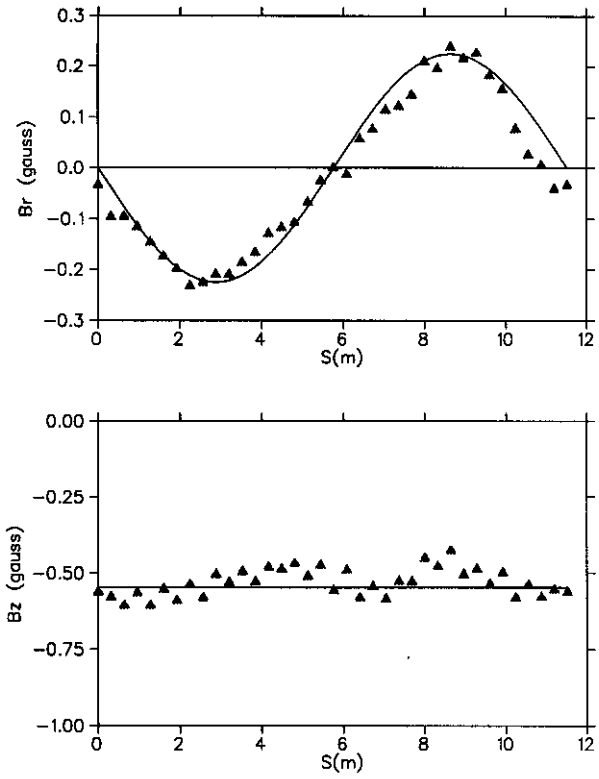

Figure 6. Earth's magnetic field. The measured data is represented by triangles and an analytical form is plotted by solid lines.

5. MISALIGNMENT AND CORRECTIONS

Misalignments of the ring magnetic elements were evaluated. The probable misalignment values estimated by the NSCL/MSU mechanical design group are given in Table 3 where Δx, Δy, Δz denote shifts in the horizontal, vertical and longitudinal directions, respectively, and $\Delta z'$ is the rotation around the z-axis. The mechanical misalignments were then represented by a Gaussian distribution with the σ values of Table 3.

Misalignment	1σ – value
Δx	0.1 mm
Δy	0.1 mm
Δz	1.0 mm
Δz'	4.0 mrad

Table 3. Mechanical misalignment values.

The mechanical misalignments result in closed orbit distortions (CODs). The correction of these CODs requires beam position monitors (BPMs) combined with active correctors in both planes. The simulated correction scheme used the readjustment of the 36 ring dipole magnets for horizontal compensation and 36 vertical correctors placed between the dipoles and quadrupoles for the vertical correction. (The vertical corrector magnetic field strengths required were <1 gauss at the injection energy assuming an effective length of 1.7 cm.)

Under these conditions (The multipole values of Table 1 and Table 2 are included. The effects of the Earth's magnetic field are not included.), the CODs as a function of BPM number was evaluated. We have explored three cases: CODs before correction, CODs after correction with 18 (one per segment) and 15 (one missing per segment) BPMs. These results are given in Table 4. The CODs around the ring for the case of 15 BPMs is given in Figure 7.

BPM #	Xmax (mm)	Ymax (mm)	Xrms (mm)	Yrms (mm)
0*	1.81	1.86	0.61	0.77
15	1.14	1.34	0.34	0.44
18	1.14	1.07	0.30	0.38

Table 4. CODs as a function of BPM number for the misalignment values of Table 3. *No BPM values are for uncorrected orbit CODs.

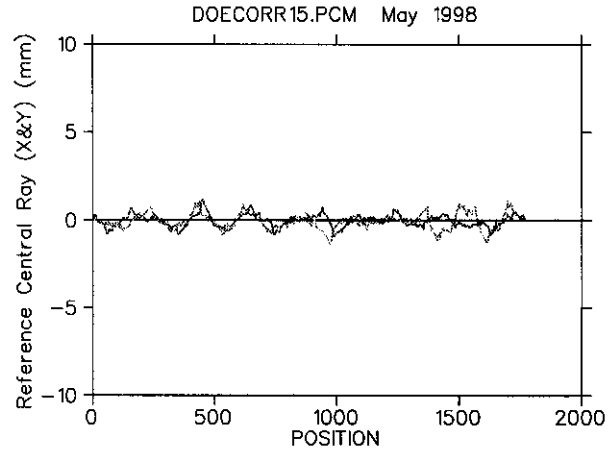

Figure 7. Closed orbit distortions due to misalignment values of Table 3 around the ring after correction with 15 BPMs.

For the case of 15 BPMs, the CODs were evaluated as a function of the misalignment values. The sigma of the Gaussian distribution was taken to be 1, 2, and 3 times the values of Table 3. The results of this evaluation are given in Table 5.

σ scale factors	Xmax (mm)	Ymax (mm)	Xrms (mm)	Yrms (mm)
1	1.14	1.34	0.34	0.44
2	2.28	2.62	0.70	0.88
3	3.43	3.84	1.08	1.32

Table 5. CODs values after correction with 15 BPMs as a function of the scaled misalignment values of Table 3.

6. MAGNET MISPOWERING

The beam dynamics will also be affected by mispowering of the ring magnetic elements. Mispowering of the dipole magnets will result in closed orbit distortions whereas quadrupole mispowering will primarily cause variation of lattice functions and tune. The mispowering which comes from the magnet power supply ripple is the primary concern in this context, and this analysis is to determine the appropriate power supply specifications in this regard.

The analysis was performed with the multipoles of Table 1 and Table 2, but no other perturbations were included. The mispowering perturbations were considered systematic. Technically the effect of mispowering was simulated by DIMAD assuming a systematic error in the momentum spread $\Delta p/p$. The CODs as a function of the dipole mispowering is given in Figure 8. The $\beta x,y$ functions variance as a function of quadrupole mispowering is given in Figure 9.

From this analysis, dipole and quadrupole power supplies with ripple specifications of 10^{-4} and 10^{-3} respectively, will provide acceptable performance.

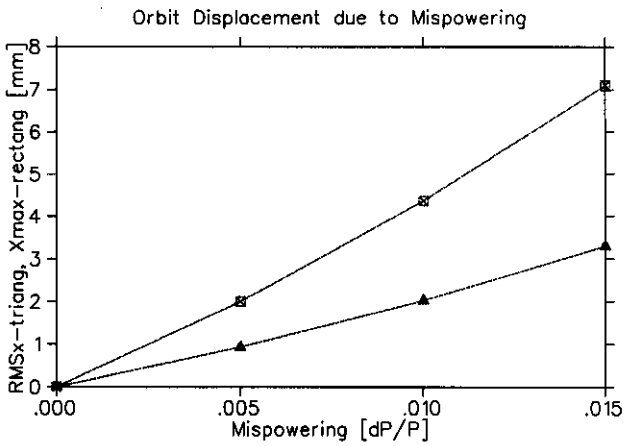

Figure 8. Orbit displacement due to dipole magnets mispowering.

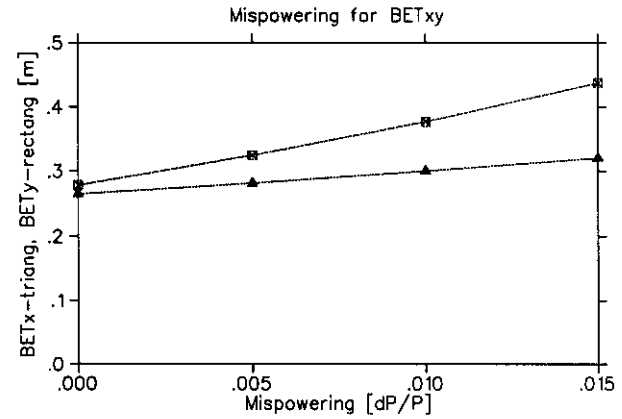

Figure 9. Lattice function distortions due to mispowering.

7. OVERALL CLOSED ORBIT DISTORTION

In the previous discussion, each lattice perturbation was considered in turn. Finally, we performed an analysis with all errors simultaneously. The errors and their values were:

- Magnet Multipoles (set at the values of Table 1 and Table 2.)
- Earth's Magnetic Fields and Corrections
- Mechanical Misalignments (set at the values of Table 3) and corrections with 15 BPMs
- Magnet Mispowering (set at 10^{-4} and 10^{-3} for the dipoles and quadrupoles respectively)

Under these conditions, we obtained CODs of:

$$\mathbf{x_{rms}=1.0\ mm,\ y_{rms}=0.47\ mm}$$
$$\mathbf{x_{max}=2.3\ mm,\ y_{max}=1.30\ mm}$$

8. DISCUSSION AND FUTURE PLANS

Based on this single particle analysis of the beam dynamics in the E-Ring we conclude that the choice of the focusing structure will provide adequate ring performance in the absence of space charge.

Nevertheless, further improvements of the focusing lattice particularly in the area of correction schemes could be of benefit. An unusual feature of the E-Ring is the significant influence of the Earth's magnetic field. The Helmholz-like wires were chosen as an efficient tool to compensate this field with a maximal current required of about 4.6 A. Though not investigated, it might be possible to utilize the corrector dipole magnets (used to correct for the mechanical misalignments) in lieu of the Helmholz-like coils.

In addition, the minimum acceptable number of BPMs might benefit from further investigation since it is anticipated that there will be significant pressure to increase the possibilities for the diagnostic hardware.

Our analysis has shown a relatively low sensitivity of the correction scheme to CO changes during optimization. The correction schemes may have been hampered by the proposed FDFD-type lattice since all BPMs are then at locations of similar β functions in both horizontal and vertical planes (see Figure 3). We have made a preliminary study of an alternative operating lattice: FDDF instead of FDFD. (Note that this simply means an alternative operating mode and its implementation requires no modification to the ring hardware.) Initial results showed an increased sensitivity to CO errors as compared to the FDDF lattice structure. As the result, it may provide a more efficient correction scheme with

fewer BPMs. However, the FDFD lattice produces machine functions a factor of five greater, and hence the beam size would be $\sqrt{5}$ =2.24 times larger as shown in Figure 10.

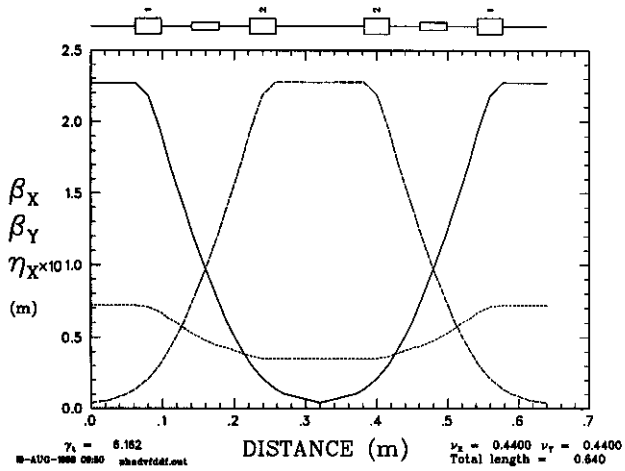

Figure 10. Alternative E-ring lattice structure. Machine functions (βx – solid, βy - dashed, ηx - dots) for one segment (2 cells).

9. REFERENCES

1 M.Reiser et al. Fusion Eng. Des. **32-33**, 293 (1996). See also: J.G.Wang, S.Bernal, P.Chin, J.J.Deng, W.Li, M.Reiser, H.Suk, M.Venturini, W.Zou, T.Godlove and R.York (1997, MDU, unpublished).

2 Users Guide to the Program DIMAD, SLAC Report 285 UC-28 (1985).

3 Physica Reference Manual, TRIUMF, Canada (1994).